Inorganic Chemistry

Article

pubs.acs.org/IC

A First-Principles Approach to the Calculation of the on-Site Zero-Field Splitting in Polynuclear Transition Metal Complexes

Marius Retegan, Nicholas Cox, Dimitrios A. Pantazis, and Frank Neese*

Max Planck Institute for Chemical Energy Conversion, Stiftstr. 34-38, 45470 Mülheim an der Ruhr, Germany

ABSTRACT: The interpretation of electron paramagnetic resonance spectra of polynuclear transition metal complexes in terms of individual contributions from each paramagnetic center can be greatly facilitated by the availability of theoretical methods that enable the reliable prediction of local spectroscopic parameters. In this work we report an approach that enables the application of multireference *ab initio* methods for the calculation of local zero field splitting tensors, one of the leading terms in the spin Hamiltonian for exchange-coupled systems of high nuclearity. The method referred to as local complete active space configuration interaction (L-CASCI) represents a multireference calculation with an active space composed of local orbitals of the center of interest. By successive permutation of the active space to include the localized orbitals corresponding to a particular center of the complex, all on-site parameters can be easily obtained at a high-level of theory with a corresponding low computational cost. Benchmark calculations on synthetic complexes confirm the validity of the approach. As an example of the applicability of the L-CASCI method to large systems, we determine the local anisotropy of the Mn(III) ion of the tetranuclear manganese cluster of photosystem II in both structural forms of its S_2 state.

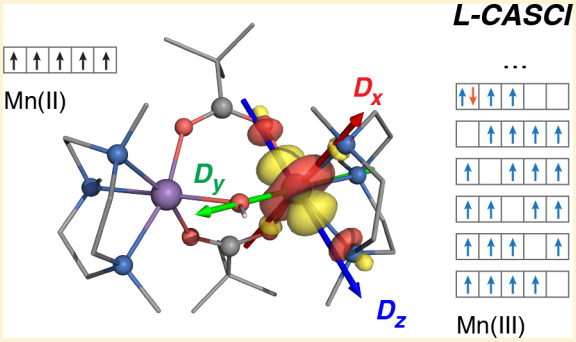

INTRODUCTION

Transition metal cluster complexes are ubiquitous in nature and synthetic chemistry, playing an enormous variety of roles ranging from multielectron catalysts[1] to single-molecule magnets. Among the techniques for characterizing them, some of the most powerful are those that probe the magnetic properties of these systems, such as electron paramagnetic resonance (EPR).[2] These methods provide important electronic structure information complementary to static spectroscopic and diffraction methods,[3] revealing, for example, the spin and oxidation state, as well as the local ligand environment of the transition metal centers.

The interpretation of EPR spectra is performed within the conceptual framework of the spin Hamiltonian formalism.[4,5] Compared to mononuclear transition metal complexes, EPR spectra of exchange-coupled polynuclear complexes are more difficult to interpret, and typically the system is described using a coupled spin Hamiltonian.[6] In this approach, the experimental spectra are fitted using a set of spectroscopic parameters that describe an "effective spin", which results from the vector-coupling of the individual spins of the system. However, by employing a coupled representation of the spin Hamiltonian, the connection with the spectroscopic parameters that refer to the individual paramagnetic centers is not usually obvious. These on-site parameters are nevertheless of central importance because they can be correlated with the local coordination environment of a given paramagnetic center, and therefore a mapping between the two representations is often sought.

Theoretical methods are increasingly being used for the calculation of magnetic and spectroscopic properties in polynuclear complexes.[7−9] Approaches based on density functional theory (DFT), such as the broken-symmetry method,[10−12] can be used to provide a more complete picture of the structural basis for the spectroscopic properties of paramagnetic ions. In previous contributions from our group we addressed some of the problems related to the calculation of these parameters in clusters of arbitrary shape and nuclearity, including a strategy for the calculation of the local hyperfine coupling (HFC) tensors from broken-symmetry DFT calculations, and their mapping to the coupled representation via a spin-projection procedure.[13−15] This has allowed us to explore correlations between structural features and spectroscopic properties for a number of synthetic and bioinorganic polynuclear clusters.[16−21]

Calculation of the local zero-field splitting (ZFS) tensors has also been the focus of recent theoretical studies.[22−26] A pragmatic approach for the calculation of this property relies on replacing all but the center of interest by diamagnetic ions with similar ionic radius, which would presumably account for the electrostatic influence of the substituted centers. In doing this the local ZFS tensor can be evaluated using methods that have been proposed for mononuclear complexes. We have recently employed this methodology to calculate the on-site anisotropy in an antiferromagnetically coupled manganese dimer,[25] while other groups have used it to estimated the local parameters for nickel- and iron-containing systems.[23,26]

Received: August 29, 2014
Published: October 23, 2014

   dx.doi.org/10.1021/ic502081c | *Inorg. Chem.* 2014, 53, 11785−11793

More rigorous approaches do not rely on diamagnetic atom substitution, but require instead modifications of the terms that enter in the expressions of the ZFS tensor. One way to achieve this is by changing the spin−orbit coupling (SOC) operator such that it only accounts for contributions originating from a single center.[22,24] Alternatively, the same terms can be expressed using localized orbitals. The local tensor is then formed by summing the contributions originating from the localized orbitals associated with that particular center.[27] However, both approaches have been limited in their implementation of DFT-based methods.

Wave function-based methods have also been used to derive local ZFS parameters. The spectroscopic parameters of the model spin Hamiltonian of a dinuclear nickel complex that included the local ZFS parameters were extracted using the effective Hamiltonian theory.[23] To account for the initial discrepancies observed in the analytical and numerical representations of the model spin Hamiltonian, higher-order operators were introduced in the model spin Hamiltonian to adequately describe the anisotropic exchange between the two centers. This, however, increases considerably the parameter space used in the fitting procedure, and makes the augmented spin Hamiltonian cumbersome to use. In the case of large systems such as the tetranuclear oxygen evolving manganese cluster of photosystem II,[28,29] or even larger systems such as the polynuclear single molecule magnets,[30] this difficulty is compounded by the enormous computational effort required for an adequate wave function-based *ab initio* description of the entire system.

Here we present a methodology for the calculation of local ZFS tensors in polynuclear metal complexes that is based on multireference *ab initio* computations performed within a localized orbital space. The approach retains the rigor and accuracy of multireference wave function-based theory, while being fast and scalable to large transition metal clusters. The method is benchmarked against experimentally characterized synthetic manganese systems of increasing nuclearity, namely, a mononuclear Mn(III) complex, a Mn(II)Mn(III) dimer, and a $Mn(IV)_2Mn(III)$ trimer. We focus on calculating the ZFS parameters of the Mn(III) ion, since significantly lower values are expected for the other oxidation states of the manganese atoms.[31−33] Following this, we use the approach to calculate the local ZFS parameters of the unique Mn(III) ion of the oxygen evolving complex of photosystem II in the S_2 state of the catalytic cycle and examine the implications of this refined description of its electronic structure for the prediction and interpretation of spectroscopic observables.

THEORETICAL BACKGROUND

The Spin Hamiltonian. In systems with more than one unpaired spin ($S > 1/2$), ZFS describes the removal of the degeneracy of the magnetic sublevels in the absence of an applied magnetic field. It is parametrized by the **D**-tensor that enters in the following phenomenological spin Hamiltonian:

$$\hat{H}_{ZFS} = \hat{S}\cdot\mathbf{D}\cdot\hat{S} \tag{1}$$

In a coordinate system that diagonalizes the tensor, the ZFS can be expressed in terms of the parameters D, E, and the tensor orientation, the former defined by

$$D = \frac{3}{2}D_{zz} \text{ and } E = \frac{1}{2}(D_{xx} - D_{yy}) \tag{2}$$

The D and E/D values are typically given in a coordinate system that fulfills the requirement of having the ratio of the E and D parameters (E/D) between 0 and 1/3.

It is often the case that for the simulation of EPR spectra the exchange-coupled system is treated as an effective mononuclear system with a total spin S. In this representation, the spin Hamiltonian that describes a particular state of interest, usually the ground state, is

$$\hat{H} = \mu_B B\cdot\mathbf{g}\cdot\hat{S} + \hat{S}\cdot\mathbf{D}\cdot\hat{S} + \sum_i^n \hat{S}\cdot\mathbf{A}'_i\cdot\hat{I}_i \tag{3}$$

Here μ_B is the Bohr magneton, B is the external magnetic field, and the first two terms represent the Zeeman and ZFS term associated with the total spin S and are parametrized by the effective **g**-matrix and **D**-tensor. The last term sums up the contributions arising from the interaction of n centers with the total spin S through a set of hyperfine coupling tensors. This representation is referred to as the coupled spin Hamiltonian.

Alternatively, the complete spin manifold for the exchange-coupled system containing n paramagnetic centers can be described by the following Hamiltonian:

$$\hat{H} = \sum_i^n (\mu_B B\cdot\mathbf{g}_i\cdot\hat{S}_i + \hat{S}_i\cdot\mathbf{D}_i\cdot\hat{S}_i + \hat{S}_i\cdot\mathbf{A}_i\cdot\hat{I}_i) - 2\sum_{i<j}^n J_{ij}\hat{S}_i\cdot\hat{S}_j \tag{4}$$

For each center the previous equation contains an electronic Zeeman term, an electron−nucleus hyperfine term, and a ZFS term. The last term of the above equation represents the exchange coupling between the centers, assumed to be isotropic in this work, the $\mathbf{g}_i$-matrix and the $\mathbf{A}_i$ and $\mathbf{D}_i$ tensors parametrize the Zeeman, hyperfine and ZFS interactions for the ith center, J_{ij} is the Heisenberg exchange coupling constant that describes the interaction between center i and j, $\hat{S}_i$ is the electron spin angular momentum operator associated with the electron magnetic moment of atom i, and $\hat{I}_i$ is the nuclear spin angular momentum operator associated with the nuclear magnetic moment of nucleus i. It is important to underline that the tensors that enter eq 3 are different from the tensors used in this uncoupled representation, and are referred to as effective tensors.

A mapping between the on-site and the effective tensors can be made on the basis of the Wigner−Eckart theorem:[6,34]

$$\mathbf{D} = \sum_i \kappa_i\mathbf{D}_i \text{ and } \mathbf{A}'_i = \rho_i\mathbf{A}_i \tag{5}$$

where κ_i and ρ_i represent weighting factors (spin-projection coefficients), defined by the spin-coupling topology of the complex of interest. In the case of the hyperfine terms, by virtue of the fact that they represent a coupling of the electron spin to the site nuclear spin, a tensor for each individual metal center is retained in the coupled representation, albeit as a scaled version of the onsite tensor. While such effective hyperfine tensors preserve the anisotropy and orientation information content of the on-site tensor, their interpretation is hampered as such effective hyperfine tensors can not be readily compared across complexes of arbitrary nuclearity. This situation is even more complex for the ZFS terms. In the coupled representation the site tensors are subsumed into a single effective tensor that, in the absence of symmetry arguments, cannot be straightforwardly decomposed. Thus, information content regarding the local properties like oxidation state and coordination geometry of the individual metal centers is essentially lost.

First-Principles Approach for the Local Anisotropy Tensors. At the multiconfigurational level, the theory for the calculation of the ZFS tensor has been described previously, and the various contributions are obtained from eqs 3−6.[35]

$$D_{KL}^{SS} = \frac{1}{2}\frac{\alpha^2}{S(2S-1)}\left\langle \Psi_0^{SS}\left|\sum_i\sum_{j\neq i}\frac{r_{ij}^2\delta_{KL} - 3(\mathbf{r}_{ij})_K(\mathbf{r}_{ij})_L}{r_{ij}^5}\right.\right.$$
$$\left.\left.\times\{2\hat{s}_{zi}\hat{s}_{zj} - \hat{s}_{xi}\hat{s}_{xj} - \hat{s}_{yi}\hat{s}_{yj}\}\right|\Psi_0^{SS}\right\rangle \quad (6)$$

$$D_{KL}^{\mathrm{SOC}-(0)} = -\frac{1}{S^2}\sum_{I'(S'=S)}\Delta_{I'}^{-1}\left\langle \Psi_0^{SS}\left|\sum_i \hat{z}_K(i)\hat{s}_0(i)\right|\Psi_{I'}^{SS}\right\rangle$$
$$\times\left\langle \Psi_{I'}^{SS}\left|\sum_i \hat{z}_L(i)\hat{s}_0(i)\right|\Psi_0^{SS}\right\rangle \quad (7)$$

$$D_{KL}^{\mathrm{SOC}-(-1)} = -\frac{1}{S(2S-1)}\times\sum_{I'(S'=S-1)}\Delta_{I'}^{-1}\left\langle \Psi_0^{SS}\left|\sum_i \hat{z}_K(i)\hat{s}_{+1}(i)\right|\right.$$
$$\left.\Psi_{I'}^{S-1S-1}\right\rangle\times\left\langle \Psi_{I'}^{S-1S-1}\left|\sum_i \hat{z}_L(i)\hat{s}_{-1}(i)\right|\Psi_0^{SS}\right\rangle \quad (8)$$

$$D_{KL}^{\mathrm{SOC}-(+1)} = -\frac{1}{(S+1)(2S+1)}\times$$
$$\sum_{I'(S'=S+1)}\Delta_{I'}^{-1}\left\langle \Psi_0^{SS}\left|\sum_i \hat{z}_K(i)\hat{s}_{-1}(i)\right|\Psi_{I'}^{S+1S+1}\right\rangle$$
$$\times\left\langle \Psi_{I'}^{S+1S+1}\left|\sum_i \hat{z}_L(i)\hat{s}_{+1}(i)\right|\Psi_0^{SS}\right\rangle \quad (9)$$

In these equations, $\Delta_{I'}$ is the energy difference between multiplet $\Psi_{I'}^{S'M'}$ and the ground state Ψ_0^{SM} in the absence of spin−orbit coupling (SOC), and $\hat{z}_K(i)$ represents the K^{th} spatial component of an effective one-electron SOC operator, in our case the spin−orbit mean-field (SOMF) operator.[36,37] The direct spin−spin coupling contribution (eq 6) is most important for organic triplet states and biradicals,[38,39] but it also plays some role for transition metal complexes.[40,41] However, for the purposes of this work it has a lesser role, and, hence, we will concentrate on the second-order SOC contribution to the ZFS, that is, Equations 7−9. It is important to stress that eqs 6−9 are exact to second-order as long as one uses exact eigenfunctions of the Born−Oppenheimer Hamiltonian in their evaluation. Thus, they hold true (to second order) no matter how high the complexity of the ground state or excited state wave functions may be in terms of spin couplings or in any other respect. Since the exact eigenfunctions required for eqs 6−9 are unobtainable and an infinite sum over states cannot be performed, it is necessary to introduce some approximations if one intends to use the equations directly.

It is evident that in addition to the actual ground-state wave function, there are contributions from potentially all excited states of the system. Given the occurrence of the energy differences in the denominator of this equations, it is also evident that the accurate determination of vertical transition energies is thus central to the calculation of reliable ZFS values. Hence, it is important to be able to calculate the relevant local d−d excited states in the presence of the other magnetic ions, to predict accurate on-site ZFS tensors. These excitation energies are sensitive functions of the local geometry around the metal center in a way that can be fully rationalized by ligand field theory.[42] A considerable complication in this respect is the complicated spin-coupling that the unpaired electrons in both the ground and the excited states undergo to couple to a given total multiplicity, a relevant quantity for evaluating eqs 7−9. The calculation of reasonably accurate excitation energies in combination with a treatment of this spin-coupling complexity is the purpose of this paper.

In the case of a polynuclear transition metal cluster, two approaches might be envisioned for the calculation of a local ZFS value, that is, the calculation of an on-site value associated with only one of the metal ions of the complex, using multiconfigurational approaches. One way would be to calculate all excited multiplets and then use a modified SOC operator such that contributions from all but one center are ignored. This is similar in spirit to the approach described recently by van Wüllen at the DFT level.[22] This "brute-force" approach, however, means that the complete electronic structure problem must be solved first, an enormous or even intractable task for a multiconfigurational *ab initio* treatment of a polynuclear cluster.

The alternative strategy presented in this work is to consider only contributions from selected excited states that are localized to the metal center of interest. Thus, the multiconfigurational calculation is constrained from the outset to yield excited states that arise exclusively from a specific metal ion, by constructing an active space from orbitals that are localized on this ion. The other ions are still present with all of their unpaired electrons, but no excitations of these "spectator electrons" are allowed. If the excitation manifold is locally complete, one may refer to this approach as the local complete active space configuration interaction (L-CASCI). The matrix elements of the SOC operator are subsequently calculated using this manifold of excited states. This approach is expected to work well if only the metal d-orbitals are in the active space, since differential dynamic correlation contributions between the ground and d−d excited states are typically small in Werner-type coordination complexes, and, hence, complete active space self-consistent field (CASSCF) (or CASCI) treatments yield good excitations energies.[43]

To arrive at the simplest possible treatment, the spins of the spectator electrons are coupled in parallel. This yields the smallest number of configuration state functions (CSFs) for a given excited-state configuration. In general, we keep all linearly independent CSFs for a given electronic configuration. Since the orbitals are localized, the exchange contributions caused by the spectator electrons are very small, as are the multicenter matrix elements of the SOC operator.

Let us illustrate the approach with a hypothetical Mn(III)/Mn(III) dimer. The active space would consist of 10 localized orbitals of which the first five are assigned to the "left" and the second five are assigned to the "right" Mn ion. If we consider the localized orbitals at each center effectively canonicalized and occurring in order of increasing energy, the ground-state configuration is given by the occupation number vector **n** = 11110[11110] (spectator electrons are in brackets). The local quintet excited states are 11101[11110], 11011[11110], 10111[11110], 01111[11110]. Since all electrons remain high-spin coupled, a total multiplicity of $S = 4$ arises for each

dx.doi.org/10.1021/ic502081c | *Inorg. Chem.* 2014, 53, 11785−11793

of these configurations, and each produces just a single CSF. For the local triplet states additional configurations like 21100[11110] arise that produce more than a single CSF of lower multiplicity that contributes to eq 7.

It is obvious that this approach is general and can, in principle, be applied to any number of transition metal ions as long as the number of linearly independent spin-couplings that arise from a given configuration stays within reasonable bounds. Since the configuration interaction (CI) calculations that are required remain very small, regardless of the number of centers, elaborate integral transformations are also not required; hence, the method is not only physically sound but also computationally attractive. Once the local SOC contribution to the ZFS is calculated using eqs 7−9, the individual contributions must be renormalized since they have been calculated on the basis of a global total spin rather than the local spin of the ion under investigation that is implied by a local ZFS tensor.

In summary, in the L-CASCI approach the electronic structure problem remains always confined to a single metal ion; therefore, the local ZFS values can be obtained directly regardless of the size of the system.

The individual steps involved in this procedure are as follows:

1) Since most of the time in an MCSCF calculation is spent in obtaining the orbitals, a convenient approach is to use initial orbitals from a restricted open-shell spin-averaged Hartree−Fock (SAHF) calculation, as described by Zerner.[44] This reduces the cost of the calculation significantly, with little effect on the final results.
2) The molecular orbitals obtained from the SAHF calculation are localized.
3) Following the assignment of the localized orbitals to individual paramagnetic centers the Fock matrix is block-diagonalized to get orbitals that are locally canonical.
4) The recanonicalized orbitals are used to build an active space that involves only the specific metal ion.
5) All CSFs at the center of interest are considered, while the other centers remain in a high-spin configuration.
6) The CI problem is solved in the basis of these CSFs.
7) The matrix elements of the SOC operator are evaluated and used to calculate the different contributions to the ZFS according to eqs 7−9.
8) The ZFS contributions are renormalized to arrive at a local ZFS tensor for the ion of interest.

To illustrate this approach, a comparison can be made to a regular MCSCF calculation. It is expected that the most significant approximations are made in the initial step that involves obtaining the orbitals. Since these orbitals are used to express the different configurations, their quality will ultimately influence the accuracy of the final ZFS parameters. This approximation can be readily tested by considering the case of a mononuclear complex (*vide infra*), since for polynuclear complexes it requires converging first a MCSCF calculation, a difficult problem as previously noted.

An important aspect in obtaining reliable ZFS parameters is the quality of the SOC operator used. Approximations to the Breit−Pauli operator have been previously considered.[37] A reliable form of the operator is based on the mean-field approximation (SOMF) to spin−orbit coupling.[36] In the present work, two further approximations are considered to the SOC operator, first by taking into account only one-center contributions to the operator, and second by replacing the molecular density used in the evaluation of the operator by the frozen density obtained from spherical atomic densities. The combination of both approximations, which is equivalent to the atomic mean-field integral (AMFI) operator developed by Schimmelpfennig, allows us to exclude specific centers from the ZFS calculation.[45] While this is not necessary here, since we take a different route in obtaining the on-site values by instead reducing the multiconfigurational space, we will also present results based on this approximation to relate our results to previously proposed DFT approaches, which do rely on such reductions of the SOC operator. As before, mononuclear complexes attest to the rigorousness of using the AMFI operator. Additionally, we consider the results obtained using the effective nuclear charge operator of Koseki, which relies on parametrized nuclear charges to approximate an effective one-electron operator.[46]

Finally, the localization of the molecular orbitals may introduce a level of ambiguity, due to the possibility of using different schemes to obtain them. For mononuclear complexes, the same values are obtained for the ZFS regardless of the localization procedure. This is not necessarily true for polynuclear complexes, and as such, the influence of a localization scheme will also be assessed in this work.

Computational Details. All calculations reported in this work were carried out with the ORCA program package.[47] For the synthetic complexes, the spectroscopic properties were calculated using structural models developed from X-ray coordinates following optimization of the hydrogen atom positions. In the case of the photosystem II models, the two S_2 state structures were taken from previously published work from our group.[19] The *ab initio* approach developed in this work for the calculation of the on-site ZFS parameters relies on obtaining molecular orbitals from a spin-averaged restricted open-shell Hartree−Fock (SAHF) calculation. For the mononuclear complexes these orbitals were also obtained from a CASSCF(4,5) calculation. The resulting orbitals were localized by minimizing their spatial extent as proposed by Foster and Boys.[48] We also tested the Pipek−Mezey[49] scheme that relies on maximizing the sum of Mulliken atomic charges to obtain the localized orbitals. Regardless of the nuclearity of the complex, the localized orbitals were easily assigned to individual paramagnetic centers. Note that the approach in general assumes the ability to assign well-defined spins to the metal centers. Following their recanonicalization, they were used to perform a local configuration interaction calculation in the space defined by the four electrons and five d orbitals of the Mn(III) ion, L-CASCI(4,5). For the mononuclear complex this reduces to a CASCI(4,5) calculation with SAHF or CASSCF orbitals. The quintet and the triplet excited states were considered when calculating the ZFS values; it has been previously shown that contributions from singlet excited states are negligible and can be safely excluded.[40] The effects of the dynamic electron correlation were evaluated using the second order *N*-electron valence perturbation theory (NEVPT2),[50,51] without any restrictions to excitations. The on-site ZFS parameters using DFT-based methods by modifying the SOC operator, in line with previous studies, were also evaluated.[22] In these calculations we tested the gradient-corrected nonhybrid functional BP86,[52,53] and we also tested the hybrid functional B3LYP with 20% exact exchange.[54] In all calculations the zeroth order regular approximation (ZORA) Hamiltonian was employed, and ZORA-recontracted versions of the def2-TZVP basis sets were used for all elements, with the exception

of the hydrogen and carbon atoms for which it was reduced to the ZORA version of def2-SVP.[55,72]

RESULTS AND DISCUSSION

Synthetic Complexes. The approach proposed in this work for the calculation of the on-site **D**-tensors was first tested on three synthetic model complexes of increasing nuclearity (Figure 1). Complex **1** is a mononuclear Mn(III) complex with

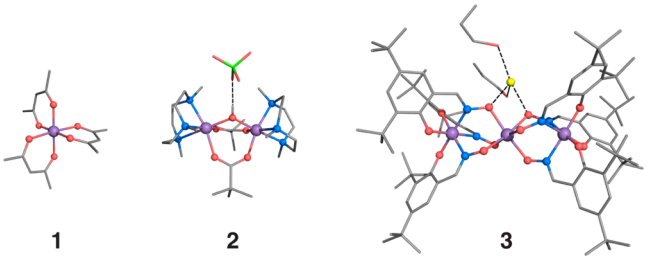

Figure 1. Structural representations of the synthetic complexes used in the present study. **1**: γ-$Mn(acac)_3$; **2**: $Mn_2(OH)(piv)_2(Me_3tacn)_2$; **3**: $NaMn_3(^tBuSao)_6$. Hydrogen atoms were omitted for clarity, with the exception of a single hydrogen atom in structure **2**.

three acetylacetone (acac) ligands.[56] Complex **2** is a Mn(II)-Mn(III) dimer where the Mn ions are bridged by one hydroxy and two carboxylato (piv) bridges, and the remaining terminal coordination sites being completed by triazacyclononane (tacn) ligands.[57] Complex **3** is a linear Mn(IV)Mn(III)Mn(IV) trimer with oximato bridges formed by salicylaldoxime (Sao) ligands.[58]

Results obtained for the mononuclear γ-$Mn(acac)_3$ complex **1** are described below. The ZFS parameters of the complex have been measured to high precision,[59] and these values are listed in Table 1. A qualitative inference can be made regarding

Table 1. Experimental and Calculated Zero-Field Splitting Parameters D (cm^{-1}) and E/D for Complex 1 at Different Levels of Theory and Different Approximations of the Spin–Orbit Coupling Operator[a]

		BP86	B3LYP	L-CASCI	CASSCF	NEVPT2
	D_{SS}	−0.40	−0.44	−0.50	−0.49	−0.49
SOMF[b]	D_{SOC}	−2.21	−2.14	−3.69	−3.62	−4.17
	D	−2.60	−2.57	−4.18	−4.11	−4.66
	E/D	0.07	0.03	0.02	0.02	0.02
AMFI[c]	D_{SOC}	−2.14	−2.08	−3.61	−3.54	−4.07
	D	−2.53	−2.51	−4.10	−4.03	−4.56
	E/D	0.07	0.03	0.02	0.02	0.02
ENC[d]	D_{SOC}	−2.03	−2.07	−3.29	−3.23	−3.72
	D	−2.42	−2.51	−3.78	−3.72	−4.21
	E/D	0.08	0.03	0.02	0.02	0.02

[a]The experimental values are D = −4.52 cm^{-1} and E/D = 0.04.[59] [b]SOMF: spin-orbit mean-field. [c]AMFI: atomic mean-field integral. [d]ENC: effective nuclear charge.

the sign of the D-parameter by considering the local environment of the high-spin metal ion. Ligand-field arguments have been previously used to link the tetragonal elongation induced by the Jahn–Teller effect to a negative value of D, while a tetragonal compression is associated with a positive D value.

As described above, the ZFS arises from both the spin–spin and spin–orbit coupling. The spin–spin contribution (D_{SS} in Table 1) to the total D value of complex **1** is essentially the same regardless of the theoretical method used, and both DFT and multiconfigurational based methods yield similar values. Moreover, it was shown using *ab initio* calculations that this contribution to the ZFS is insensitive to the coordination environment of the metal ion.[32] It is thus expected that the spin–spin contribution to the on-site ZFS tensor will remain the same for a single Mn(III) ion in polynuclear systems, and will therefore not be considered in the following discussion regarding the dimer and trimer synthetic complexes.

In line with previous observations regarding mononuclear Mn(III) complexes, the calculated value at the DFT level of theory using the elaborate SOMF operator underestimates the magnitude of spin–orbit coupling (D_{SOC}) regardless of the functional used.[32] For both functionals tested here we calculate a value approximately 40% smaller than experimental results. Larger deviations were observed for the in-plane anisotropy, that is, the E/D parameter, with a more rhombic ZFS calculated using the BP86 functional.

The two multiconfigurational methods presented here (L-CASCI and CASSCF) achieve much better agreement with experiment. We stress again that the only difference between the two methods is the nature of the orbitals used in the configuration interaction treatment. In the CASSCF calculation, they are averaged orbitals over the quintet and triplet states, while for the L-CASCI approach, they are obtained from a SAHF calculation averaged over all high-spin configurations. This explains why the two approaches give slightly different D values. The E/D parameter is consistently reproduced using both approaches, and compares very well with the experimentally determined value. In terms of cost, we note that for the present system the cost of generating CASSCF orbitals is more than 10 times that of generating SAHF orbitals.

Next we focus on the performance of less elaborate SOC operators and the effect of the additional approximations they introduce. In neglecting multicenter terms for the spin–orbit coupling part of the D tensor, the two SOC operators defined in the Theoretical Background section (AMFI and ENC) allow for a rigorous separation into site contributions. The results of these approximations are presented in Table 1. It can be seen that the AMFI operator, which in addition relies on spherical atomic densities to build the molecular electron density, is a very good approximation to the calculation of SOC. At all levels of theory approximately 98% of the SOMF results are recovered, with less than 0.1 cm^{-1} difference in absolute value.

In the case of the parametrized effective nuclear charge operator (ENC), the SOC contributions are also consistently underestimated. In this case, however, the difference compared with the SOMF operator is more significant and amounts to an underestimation of approximately 10% of the total value, an error which is known to increase as a function of atomic number. Even so, applying the ENC operator to multiconfigurational wave functions still provides a better estimate of the ZFS parameters when compared with DFT results. This is true even when a more accurate SOC operator is used with DFT; that is, the error that originates from the use of DFT is greater than the error originating from approximate expressions of the SOC operator.

Multiconfigurational methods provide the basis for further improving the quality of the predictions. This is also the case for this type of system, for which it has been shown that inclusion of dynamical correlation either by perturbative or variational approaches can improve the calculated values.

dx.doi.org/10.1021/ic502081c | Inorg. Chem. 2014, 53, 11785–11793

Indeed, by using *N*-electron valence perturbation theory on top of the CASSCF wave function, the values for D_{SOC} improve by approximately 10%.[32] This trend was also observed for a set of Mn(III) complexes, for which the standard deviation between the experimental and calculated values was improved by including dynamical correlation. In this case, however, the improvement was modest, less than 5%, suggesting that considering only the static correlation is sufficient on average for the calculation of accurate ZFS parameters for the type of systems studied here.

A quantitative picture regarding the approximations introduced by L-CASCI compared to CASSCF and the effect of dynamic electron correlation results from the comparison of the vertical ligand-field transition energies obtained using different methods. The correct evaluation of these transition energies is of central importance in calculating the ZFS parameters, since the values enter in the denominator of eqs 6−9 and also determine the amount of state mixing. As shown in Table 2, essentially the same values are obtained for L-CASCI and CASSCF, with the differences never exceeding 500 cm^{-1}. The inclusion of dynamic correlation using the NEVPT2 method improves the quality of the calculated transition energies, which results in the better agreement seen previously for the calculated *D* value and experiment.

Table 2. Comparison of Calculated and Experimental Vertical Transition Energies (cm^{-1}) for Complex 1.

transition[a]	L-CASCI	CASSCF	NEVPT2	expt
$^5E_g \rightarrow {}^5E_g$	6960	7010	7900	9520
$^5E_g \rightarrow {}^5T_{2g}$	16 460	16 540	19 940	17 900
	17 810	17 920	21 390	21 500
	18 220	18 360	22 130	21 500
$^5E_g \rightarrow {}^3T_{2g}$	15 120	14 700	10 140	
	15 190	14 770	10 400	
	16 130	15 720	11 630	

[a] O_h symmetry labels are used to describe the transitions.

It is clear from the above discussion that the inability of DFT methods to quantitatively predict the *D* value is due to an underestimation of the SOC contribution. This suggests that a DFT-based procedure to obtain local ZFS parameters would be complicated by intrinsic deficiencies of the method for this type of property. On the other hand, the accuracy of the predictions when using SAHF orbitals to avoid a costly MCSCF calculation, establishes the L-CASCI method as a viable alternative to the CASSCF method. Moreover, the results obtained using multiconfigurational approaches can be systematically improved, while no clear route can be envisaged for DFT methods. Here both functionals underestimate the experimental value by the same amount. This result should not, however, be extrapolated to other functionals, for which unsystematic variations were obtained in the case of other Mn(III) containing systems,[32] or to other paramagnetic systems where DFT-based methods were shown to fail entirely.[60−62]

Having confirmed the reliability of the L-CASCI approach for the mononuclear system, we apply the procedure outlined in the methodology section to the dinuclear complex **2**. Note that the size of the dinuclear complex is already large enough to render MCSCF calculations on the complete system challenging. This is not only because of the expansion of the active space but also because of the explosive increase in the number of required states that must be computed to include all relevant excitations from all metal centers of interest. By contrast, the L-CASCI approach always involves computing a strictly limited number of only the necessary roots for a single metal center, regardless of the nuclearity of the complex. In the case of the Mn(III) ion, for instance, only 50 roots need to be computed always, instead of more than 18 000 roots required for a complete CAS(9,10) treatment of the dinuclear system.

Table 3 shows that good agreement is achieved between the L-CASCI values and the experimental estimate made by mapping the spin Hamiltonian parameters to the on-site values. DFT again grossly underestimates the absolute value of the SOC contribution regardless of the density functional used. Using a similar approach for the calculation of the on-site ZFS at the DFT level, a similar underestimation was observed in the case of other dinuclear complexes.[24] To arrive at an agreement with experimental values an artificial prefactor of 3 had been used by Schraut et al.[24] to correct the calculated on-site ZFS values of the Mn(III). Moreover, a stark qualitative difference is observed in the results obtained with the two different functionals, since using the AMFI operator B3LYP predicts a positive value of D_{SOC} for complex **2**, most probably due to the large *E*/*D* value.

Table 3. Calculated Spin-Orbit Coupling Contributions to the Zero-Field Splitting Parameters for the Mn(III) Ion in Complexes 2 and 3 Using Different Levels of Theory

			BP86	B3LYP	L-CASCI
2[a]	AMFI	D_{SOC}	−0.99	1.49	−3.04
		E/*D*	0.29	0.32	0.25
	ENC	D_{SOC}	−0.91	−1.36	−2.73
		E/*D*	0.27	0.30	0.25
3	AMFI	D_{SOC}	1.50	3.24	3.12
		E/*D*	0.04	0.02	0.01
	ENC	D_{SOC}	1.41	2.49	2.82
		E/*D*	0.04	0.01	0.01

[a] The experimental values for **2** are $D = -3.72\ cm^{-1}$ and $E/D = 0.31$.[63]

To test the influence of the localization scheme used to obtained the orbitals we compare the Foster−Boys and the Pipek−Mezey localization schemes for the dimer system. Even though the two localization schemes are formally distinct, they produce very similar orbitals. Since the localized nature of the orbitals is maintained in the following recanonicalization procedure, as illustrated by the plots in Figure 2, it is not surprising that the same value is obtained for the on-site ZFS parameters using two distinct sets of orbitals to build the active space in the L-CASCI method.

Experimental data for complex **3** is restricted to the sign of the local ZFS parameter, which is positive due to the compressed coordination environment of the central Mn(III) ion.[58] All methods (Table 3) manage to reproduce the sign of *D*. However, the results confirm the inconsistent and unpredictable behavior of DFT, since B3LYP yields a *D* value that is in agreement with the L-CASCI results, whereas BP86 underestimates this value by a factor of 2.

Application to the Oxygen Evolving Complex. The results on the synthetic complexes presented above confirm the accuracy and efficiency of the L-CASCI approach. As a demonstration of how this method can be readily applied to systems of even higher nuclearity, we present below calculations on the catalytic site of water oxidation, termed

dx.doi.org/10.1021/ic502081c | Inorg. Chem. 2014, 53, 11785−11793

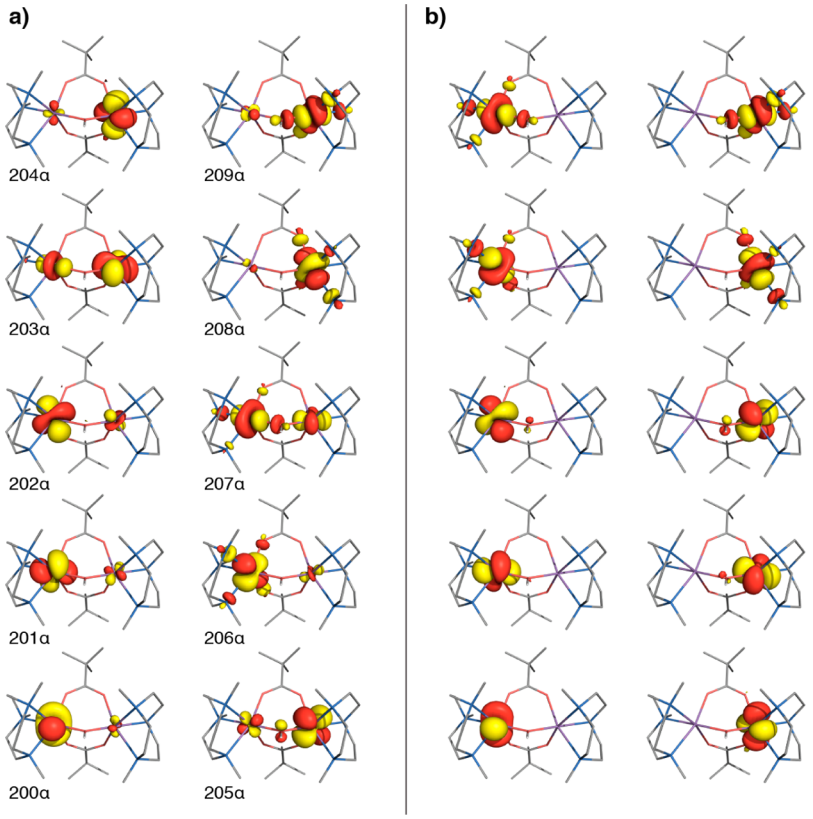

Figure 2. (a) Canonical orbitals of complex **2** obtained from a SAHF calculation. (b) Foster−Boys localized and recanonicalized orbitals used in the L-CASCI approach.

the oxygen-evolving complex (OEC), of photosystem II. The OEC contains a cluster of four manganese ions and one calcium ion connected through a network of five μ-oxo bridges that facilitate the exchange coupling between the manganese centers.[64] The cluster passes through a series of five metastable intermediate states during its reaction cycle[65] called the S_i states (i = 0−4) where the subscript denotes the number of stored oxidizing equivalents required for the four-electron water-splitting reaction.

The S_2 state, which is the most extensively characterized state by magnetic resonance spectroscopies,[66−71] represents a net oxidation state of the complex of $Mn(IV)_3Mn(III)$. Combined spectroscopic and computational efforts established that S_2 displays two discrete ground states, namely, a low-spin (S = 1/2) and a high-spin state (S = 5/2) that represent two discrete structural conformations of the cluster, called S_2^A and S_2^B, related by relocation of the only Mn(III) ion of the cluster (see Figure 3).[19] Crucially, in both the low- and the high-spin conformations of the S_2 state, the ZFS of the Mn(III) ion determines the anisotropy of the whole complex.

In the high-spin configuration (S = 5/2), the site ZFS of the Mn(III) is expected to define the total ZFS of the ground electronic state of the complex (D_S) and thus the spectral shape of the EPR envelope and the position of the only resolved turning point seen using X-band, the $g \geq 4.1$ seen at ca. 160 mT (ν = 9.4 GHz). This is because the three Mn(IV) ions of the complex display much smaller site ZFS splitting (computed values on the order of 0.2 cm^{-1}) and as such do not need to be considered. In the low-spin (S = 1/2) conformation, the effect of the fine structure value of the Mn(III) ion on the ground electronic state is indirect: as the ground state is not well

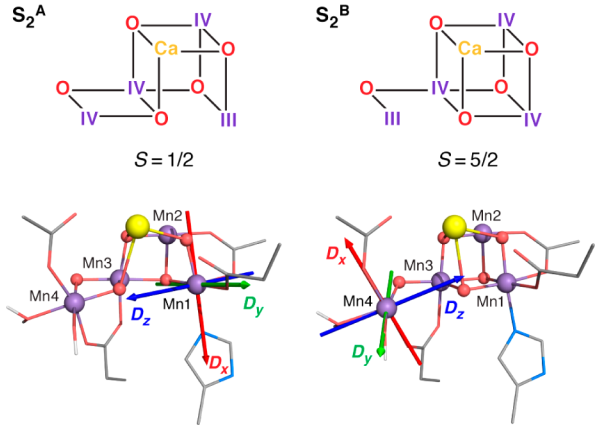

Figure 3. (upper) Schematic representation of the Mn oxidation state distribution in the two interconvertible forms of the S_2 state of the OEC. (lower) Orientation of the principal axes of the D_{SOC} for the five-coordinate Mn(III) ion in each S_2 conformation.

isolated, excited spin state character is mixed into the ground state, perturbing its measured magnetic properties and defining the large g and ^{55}Mn hyperfine anisotropy of the system.[19]

Theoretical approaches are necessary to maximize the information content of the rich but complicated EPR spectra, but these approaches up to the present point have been limited to DFT-based methodologies. Here we attempt L-CASCI calculations to determine the local anisotropy of the unique Mn(III) ion in the S_2 state of the OEC. This is the first time this level of theory is applied to a system of such size.

Following the L-CASCI procedure outlined above, we calculated the SOC contribution to the D tensor of Mn(III)

dx.doi.org/10.1021/ic502081c | Inorg. Chem. 2014, 53, 11785−11793

in the two S_2 state conformations. The computed values for D_{SOC} are −3.67 and −3.06 cm^{-1} for the S_2^A and S_2^B forms, respectively. These values agree well with estimates from current literature.[70,71] The total ZFS of the S_2^B isomer was estimated via multifrequency EPR measurements and complementary static magnetization (SQUID) measurements to be ca. 0.5 cm^{-1}, which would map to a Mn(III) site ZFS of ca. 3 cm^{-1}. Similarly, the site ZFS of the Mn(III) ion of the S_2^A isomer was inferred from the measured hyperfine anisotropy of the four Mn ions. As noted above, because the ground spin state is not well isolated, the anisotropic component of the effective hyperfine tensors used to simulate the low-spin EPR spectrum is taken as a measure for the site ZFS of the Mn(III) ion. This value has not been inferred experimentally except from a lower bound of approximately −1.5 cm^{-1},[19] which is strongly dependent on the precise magnetic (exchange) interactions within the complex. It is more likely, as the theoretical calculations show, that the site ZFS for the unique Mn(III) in each of the S_2 state isomers is similar, consistent with the similar coordination geometry of the Mn(III) ion in both structures. Since the method permits the calculation of the full **D**-tensor, it also allows access to the orientation of the principal components of the tensor. As shown in Figure 3, the D_z component for both conformers is oriented along the open coordination site of the Mn(III) ion.

The implications of these results for interpreting specific magnetic resonance data on the S_2 state and for elucidating the details of the progression to the next step of the catalytic cycle (S_3)[73] will not be pursued here. At this point we simply wish to note that the method presented in this work allows, for the first time, access to such local parameters for polynuclear systems, bioinorganic as well as synthetic, at a level of multireference theory that overcomes the limitations of single-determinant methods like those of DFT.

CONCLUSIONS

A method is proposed for calculating the local ZFS parameters in polynuclear transition metal complexes using a multireference approach. The method is based on defining a reference active space that is constructed only from orbitals localized on the metal ion of interest. This approach enables application of high-level wave function-based *ab initio* methods for the prediction of local (on-site) spectroscopic parameters that enter in the uncoupled representation of the spin Hamiltonian. In this way, it can be ensured that ambiguities and intrinsic deficiencies of DFT approaches are avoided, while at the same time no artificial chemical modification of the model is introduced, as in the case of the atom substitution approach. The method described above was tested on a series of synthetic complexes to validate its performance. Subsequently, it is successfully applied to the oxygen-evolving Mn_4CaO_5 cluster of photosystem II, a large spin-coupled system that is typical of the intended applications of the method. The present work forms the basis for rigorous multireference *ab initio* studies of exchange-coupled systems containing multiple centers with potentially large and noncollinear local anisotropies.

AUTHOR INFORMATION

Corresponding Author

*E-mail: frank.neese@cec.mpg.de.

Notes

The authors declare no competing financial interest.

REFERENCES

(1) *Metal Ions in Life Sciences*; Sigel, A., Sigel, H., Sigel, K. O., Eds.; John Wiley & Sons, Ltd.: Chichester, West Sussex, U.K., 2006−2013; Vols. *1*−*12*.
(2) Abragram, A.; Bleaney, B. *Electron Paramagnetic Resonance of Transition Metal Ions;* Clarendon Press: Oxford, U.K., 1970.
(3) *Inorganic Electronic Structure and Spectroscopy;* Solomon, E. I.; Lever, A. B. P., Eds.; John Wiley & Sons, Inc.: Chichester, West Sussex, U.K., 1999; Vols. *I*−*II*.
(4) Neese, F.; Solomon, E. I. Interpretation and Calculation of Spin-Hamiltonian Parameters in Transition Metal Complexes. In *Magnetism: Molecules to Materials IV;* Miller, J. S., Drillon, M., Eds.; Wiley-VCH Verlag GmbH & Co. KGaA: Weinheim, Germany, 2003; pp 345−466.
(5) Neese, F. Quantum Chemical Approaches to Spin-Hamiltonian Parameters. In *Electron Paramagnetic Resonance;* Gilbert, B. C., Davies, M. B., Murphy, D. M., Eds.; Royal Society of Chemistry: Cambridge, U.K., 2007; Vol. *20*, pp 73−95.
(6) Bencini, A.; Gatteschi, D. *EPR of Exchange Coupled Systems;* Springer-Verlag: Berlin, Germany, 1990.
(7) Neese, F. *Coord. Chem. Rev.* **2009**, *253*, 526−563.
(8) Helgaker, T.; Coriani, S.; Jørgensen, P.; Kristensen, K.; Olsen, J.; Ruud, K. *Chem. Rev.* **2012**, *112*, 543−631.
(9) Malrieu, J. P.; Caballol, R.; Calzado, C. J.; de Graaf, C.; Guihéry, N. *Chem. Rev.* **2014**, *114*, 429−492.
(10) Noodleman, L. *J. Chem. Phys.* **1981**, *74*, 5737.
(11) Noodleman, L.; Davidson, E. R. *Chem. Phys.* **1986**, *109*, 131−143.
(12) Caballol, R.; Castell, O.; Illas, F.; Moreira, I. de P. R.; Malrieu, J. P. *J. Phys. Chem. A* **1997**, *101*, 7860−7866.
(13) Pantazis, D. A.; Orio, M.; Petrenko, T.; Zein, S.; Bill, E.; Lubitz, W.; Messinger, J.; Neese, F. *Chem.—Eur. J.* **2009**, *15*, 5108−5123.
(14) Orio, M.; Pantazis, D. A.; Petrenko, T.; Neese, F. *Inorg. Chem.* **2009**, *48*, 7251−7260.
(15) Pantazis, D. A.; Krewald, V.; Orio, M.; Neese, F. *Dalton Trans.* **2010**, *39*, 4959−4967.
(16) Baffert, C.; Orio, M.; Pantazis, D. A.; Duboc, C.; Blackman, A. G.; Blondin, G.; Neese, F.; Deronzier, A.; Collomb, M.-N. *Inorg. Chem.* **2009**, *48*, 10281−10288.
(17) Pantazis, D. A.; Orio, M.; Petrenko, T.; Zein, S.; Lubitz, W.; Messinger, J.; Neese, F. *Phys. Chem. Chem. Phys.* **2009**, *11*, 6788−6798.
(18) Ames, W.; Pantazis, D. A.; Krewald, V.; Cox, N.; Messinger, J.; Lubitz, W.; Neese, F. *J. Am. Chem. Soc.* **2011**, *133*, 19743−19757.
(19) Pantazis, D. A.; Ames, W.; Cox, N.; Lubitz, W.; Neese, F. *Angew. Chem., Int. Ed.* **2012**, *51*, 9935−9940.
(20) Retegan, M.; Neese, F.; Pantazis, D. A. *J. Chem. Theory Comput.* **2013**, *9*, 3832−3842.
(21) Krewald, V.; Neese, F.; Pantazis, D. A. *J. Am. Chem. Soc.* **2013**, *135*, 5726−5739.
(22) van Wüllen, C. *J. Phys. Chem. A* **2009**, *113*, 11535−11540.
(23) Maurice, R.; Guihéry, N.; Bastardis, R.; de Graaf, C. *J. Chem. Theory Comput.* **2010**, *6*, 55−65.
(24) Schraut, J.; Arbuznikov, A. V.; Schinzel, S.; Kaupp, M. *ChemPhysChem* **2011**, *12*, 3170−3179.
(25) Retegan, M.; Collomb, M.-N.; Neese, F.; Duboc, C. *Phys. Chem. Chem. Phys.* **2013**, *15*, 223−234.
(26) Maurice, R.; Verma, P.; Zadrozny, J. M.; Luo, S.; Borycz, J.; Long, J. R.; Truhlar, D. G.; Gagliardi, L. *Inorg. Chem.* **2013**, *52*, 9379−9389.
(27) Kessler, E. M. V.; Schmitt, S.; van Wüllen, C. *J. Chem. Phys.* **2013**, *139*, 184110.
(28) Cox, N.; Pantazis, D. A.; Neese, F.; Lubitz, W. *Acc. Chem. Res.* **2013**, *46*, 1588−1596.
(29) Pantazis, D. A.; Cox, N.; Lubitz, W.; Neese, F. *Encyclopedia of Inorganic and Bioinorganic Chemistry* 2014, *online edition*, 10.1002/9781119951438.eibc2166.

(30) Gatteschi, D.; Sessoli, R. *Angew. Chem., Int. Ed.* **2003**, *42*, 268−297.
(31) Duboc, C.; Collomb, M.-N.. *Chem. Commun.* **2009**, 2715−2717.
(32) Duboc, C.; Ganyushin, D.; Sivalingam, K.; Collomb, M.-N.; Neese, F. *J. Phys. Chem. A* **2010**, *114*, 10750−10758.
(33) Bane, K.; Geiger, R. A.; Chabolla, S. A.; Jackson, T. A. *Inorg. Chim. Acta* **2012**, *380*, 135−140.
(34) Sage, J. T.; Xia, Y. M.; Debrunner, P. G.; Keough, D. T.; De Jersey, J.; Zerner, B. *J. Am. Chem. Soc.* **1989**, *111*, 7239−7247.
(35) Neese, F.; Solomon, E. I. *Inorg. Chem.* **1998**, *37*, 6568−6582.
(36) Hess, B. A.; Marian, C. M.; Wahlgren, U.; Gropen, O. *Chem. Phys. Lett.* **1996**, *251*, 365−371.
(37) Neese, F. *J. Chem. Phys.* **2005**, *122*, 034107.
(38) Vahtras, O.; Loboda, O.; Minaev, B.; Ågren, H.; Ruud, K. *Chem. Phys.* **2002**, *279*, 133−142.
(39) Sinnecker, S.; Neese, F. *J. Phys. Chem. A* **2006**, *110*, 12267−12275.
(40) Neese, F. *J. Am. Chem. Soc.* **2006**, *128*, 10213−10222.
(41) Liakos, D. G.; Ganyushin, D.; Neese, F. *Inorg. Chem.* **2009**, *48*, 10572−10580.
(42) Atanasov, M.; Ganyushin, D.; Sivalingam, K.; Neese, F. A Modern First-Principles View on Ligand Field Theory Through the Eyes of Correlated Multireference Wavefunctions. In *Molecular Electronic Structures of Transition Metal Complexes II;* Mingos, D. M. P., Day, P., Dahl, J. P., Eds.; Springer: Berlin, Heidelberg, 2012; Vol. *143*, pp 149−220.
(43) Neese, F.; Petrenko, T.; Ganyushin, D.; Olbrich, G. *Coord. Chem. Rev.* **2007**, *251*, 288−327.
(44) Stavrev, K. K.; Zerner, M. C. *Int. J. Quantum Chem.* **1997**, *65*, 877−884.
(45) Iliaš, M.; Kellö, V.; Visscher, L.; Schimmelpfennig, B. *J. Chem. Phys.* **2001**, *115*, 9667.
(46) Koseki, S.; Schmidt, M. W.; Gordon, M. S. *J. Phys. Chem.* **1992**, *96*, 10768−10772.
(47) Neese, F. *Wiley Interdiscip. Rev.: Comput. Mol. Sci.* **2012**, *2*, 73−78.
(48) Foster, J.; Boys, S. *Rev. Mod. Phys.* **1960**, *32*, 300−302.
(49) Pipek, J.; Mezey, P. G. *J. Chem. Phys.* **1989**, *90*, 4916.
(50) Angeli, C.; Cimiraglia, R.; Malrieu, J.-P. *J. Chem. Phys.* **2002**, *117*, 9138.
(51) Angeli, C.; Cimiraglia, R.; Malrieu, J.-P. *Theor. Chem. Acc.* **2006**, *116*, 434−439.
(52) Becke, A. D. *Phys. Rev. A* **1988**, *38*, 3098−3100.
(53) Perdew, J. *Phys. Rev. B* **1986**, *33*, 8822−8824.
(54) Becke, A. D. *J. Chem. Phys.* **1993**, *98*, 1372.
(55) Pantazis, D. A.; Chen, X.-Y.; Landis, C. R.; Neese, F. *J. Chem. Theory Comput.* **2008**, *4*, 908−919.
(56) Stults, B. R.; Marianelli, R. S.; Day, V. W. *Inorg. Chem.* **1979**, *18*, 1853−1858.
(57) Bossek, U.; Hummel, H.; Weyhermüller, T.; Wieghardt, K.; Russell, S.; van der Wolf, L.; Kolb, U. *Angew. Chem., Int. Ed. Engl.* **1996**, *35*, 1552−1554.
(58) Zhou, C.-L.; Wang, Z.-M.; Wang, B.-W.; Gao, S. *Dalton Trans.* **2012**, *41*, 13620−13625.
(59) Krzystek, J.; Yeagle, G. J.; Park, J.-H.; Britt, R. D.; Meisel, M. W.; Brunel, L.-C.; Telser, J. *Inorg. Chem.* **2003**, *42*, 4610−4618.
(60) Maganas, D.; Sottini, S.; Kyritsis, P.; Groenen, E. J. J.; Neese, F. *Inorg. Chem.* **2011**, *50*, 8741−8754.
(61) Ye, S.; Neese, F. *J. Chem. Theory Comput.* **2012**, *8*, 2344−2351.
(62) Maganas, D.; Krzystek, J.; Ferentinos, E.; Whyte, A. M.; Robertson, N.; Psycharis, V.; Terzis, A.; Neese, F.; Kyritsis, P. *Inorg. Chem.* **2012**, *51*, 7218−7231.
(63) Cox, N.; Ames, W.; Epel, B.; Kulik, L. V.; Rapatskiy, L.; Neese, F.; Messinger, J.; Wieghardt, K.; Lubitz, W. *Inorg. Chem.* **2011**, *50*, 8238−8251.
(64) Umena, Y.; Kawakami, K.; Shen, J.-R.; Kamiya, N. *Nature* **2011**, *473*, 55−60.
(65) Kok, B.; Forbush, B.; McGloin, M. *Photochem. Photobiol.* **1970**, *11*, 457−475.
(66) Dismukes, G. C.; Siderer, Y. *Proc. Natl. Acad. Sci. U.S.A.* **1981**, *78*, 274−278.
(67) Boussac, A.; Girerd, J.-J.; Rutherford, A. W. *Biochemistry* **1996**, *35*, 6984−6989.
(68) Messinger, J.; Robblee, J. H.; Yu, W. O.; Sauer, K.; Yachandra, V. K.; Klein, M. P. *J. Am. Chem. Soc.* **1997**, *119*, 11349−11350.
(69) Åhrling, K. A.; Peterson, S.; Styring, S. *Biochemistry* **1997**, *36*, 13148−13152.
(70) Horner, O.; Rivière, E.; Blondin, G.; Un, S.; Rutherford, A. W.; Girerd, J.-J.; Boussac, A. *J. Am. Chem. Soc.* **1998**, *120*, 7924−7928.
(71) Haddy, A.; Lakshmi, K. V.; Brudvig, G. W.; Frank, H. A. *Biophys. J.* **2004**, *87*, 2885−2896.
(72) Weigend, F.; Ahlrichs, R. *Phys. Chem. Chem. Phys.* **2005**, *7*, 3297−3305.
(73) Cox, N.; Retegan, M.; Neese, F.; Pantazis, D. A.; Boussac, A.; Lubitz, W. *Science* **2014**, *345*, 804−808.